Eur. Phys. J. B **9**, 59–69 (1999)

THE EUROPEAN PHYSICAL JOURNAL B

EDP Sciences
© Società Italiana di Fisica
Springer-Verlag 1999

Compression of a soft sphere packing

T. Lachhab[1] and C. Weill[2,a]

[1] Faculté des Sciences Hassan II Ben M'sick, Département de Physique, Boulevard Idriss el Harti, Casablanca, Morocco
[2] UMR 113, 2 Allée Képler, 77420 Champs sur Marne, France

Received 27 January 1998

Abstract. Mechanical properties of packings of deformable spheres of polyelectrolyte gel are studied experimentally. These particles are plunged into a brine. They have the property to swell and shrink when the concentration of salt of the solution is varied. An oedometric compression is performed imposing cycles of deformation at constant speed and constant salinity C_s. Under many different conditions, we study the laws of deformation relating the macroscopic compression force F, to the macroscopic strain ε. We find empirical non linear relations of the type $F \sim \varepsilon^m$. The values of this exponent m are discussed and compared to the results of measurements on a single sphere compressed on a plane as well as to the results of experiments and simulations on dry model granular assemblies. The swelling and deswelling properties of the spheres are used to perform isotropic compression tests. In this situation we determine the relation between the force at equilibrium and the macroscopic strain $\varepsilon(C_s)$. The results are compared with those obtained in the oedometric compression tests.

PACS. 81.40.Jj Elasticity and anelasticity, stress-strain relations – 83.70.Fn Granular solids – 82.70.Gg Gels and sols

1 Introduction

Granular matter is present in numerous practical situations ranging from natural assemblies of sand in the desert, sediments in the rivers, to industrial pastes involved into numerous fabrication processes [1]. An important issue is still the elaboration of an unified mechanical picture describing the static or the quasi-static behavior of large assemblies of grains with or without a surrounding fluid [2,3]. So far, a very partial knowledge of this problem has been achieved for which the consequences are very practical. For example, the numerous incidents observed in industrial production lines when changing even slightly the operation modes or the still unexplained collapses occurring repetidly in industrial silos, can be attributed to this ignorance. One of the big challenge is to achieve a description where the knowledge of local interactions between the grains allows to make a prediction at a collective level. The difficulty in this passage to a macroscopic description, is to understand the emergence of collective behaviors such as vault effects, global reorganizations, contact dynamics *etc.* Recently, the problem of force transmission has generated many contributions either experimental [4–6], numerical [7–9] or theoretical [10,11]; essentially the problem of a dry granular assembly was investigated. These studies have shown that the problem of force transmission is indeed a difficult one, and propositions were made that new concepts of disordered systems borrowed from statistical physics could be applied there. This activity generates an active debate between communities interested by granular matter, namely, in physics, soil mechanics [12], civil engineering [13], *etc.* Nevertheless, in any case, it seems that for such complex systems the study of model granular assemblies is crucial since it focuses experimental and theoretical works on systems which are simple enough to expect an unified vision. For example, in the case of dry granular assemblies, early experiments of photoelasticity performed on disordered compressed packings of discs [38] and spheres [39] have shown the heterogeneous character of the network of stressed particles and the large range of contact forces. More recently, model experiments of compression coupled with photoelastic observations have been made on bidimensional ordered and disordered packings of cylinders [6,14]; those studies have stressed on the importance of the contact dynamics during the compression process and have also visualized the resulting heterogeneities of the stress path; in this situation, the macroscopic compression laws are found to be influenced by both the local interactions laws, the contact dynamics, and the possible emergence of long range structures in the form of force chains spanning the whole system. In the case of granular assemblies embedded in a fluid, their mechanical properties will depend essentially on the interactions between the particles and on their size. In colloidal suspensions, long range electrostatic interactions can generate ordered structures. Such systems behave like ductile solids, exhibiting a non zero shear modulus and a yield

[a] e-mail: claire-weill@mies.premier-ministre.gouv.fr

stress (although very low) when submitted to a shear [15]. When the interactions between colloidal particles are of short range (van der Waals forces), the particles tend to stick and to form aggregates. If these aggregates become sufficiently large, they can settle under their own weight. Hence, the deformation induced by gravity of large gel molecules [16], as well as on aggregated colloidal suspensions has been observed. In the second situation, a recent experiment [17] has also shown that this deformation can saturates when the initial height of the sample increases. This striking effect is due to the friction of the aggregates with the walls of the cell and is reminiscent of Janssen's law for dry granular assemblies in a silo. In concentrated suspensions of deformable particles, the friction forces of lubricated nature are very reduced compare to solid friction. Understanding the rheology of such systems is of great practical importance in food industry, as well as in cosmetical and pharmaceutical industry; it is also of great scientific interest. Recently, some experimental work has been devoted to the study of the rheological properties of concentrated suspensions of gel beads [40,41]. In this article, we design a model tridimensional granular medium made of an assembly of compressible spheres of millimetric size embedded in an aqueous solvent. The particles are polyelectrolyte gels swollen in brine (salty water). Two original properties of this system are used. (i) The particles have the possibility to swell a large amount in salty water (for concentrations of salt $C_s > 100$ g/l) and consequently, their density is very close to one. This effect considerably reduces the role of gravity in the packing which is initially isotropic. (ii) The size of the particles varies reversibly with the salt concentration. This last property allows to perform real experiments of isotropic compression, where the particles successively swell and shrink. Finally, since the particles are very deformable and the friction between them not very high, this procedure allows much more rearrangements in the piling than for rigid and rough particles and therefore, allows us to explore many different regimes of compression. In this report, two kinds of experiments are performed: oedometric compression at a constant salinity and at a constant deformation speed and then, isotropic compression in the quasistatic regime by varying the salinity of the aqueous solution.

This paper is organized as follows: in Section 2 we briefly recall the theory of the mechanical contact between two spheres (local law). The Section 3 is devoted to the study of the mechanical behavior of packings under odeometric compression. The isotropic compression experiments are presented and analyzed in Section 4.

2 Theory: contact laws

Let us consider two elastic spheres in contact and submitted to an external normal force f. Due to the fact that the surface of contact between the two spheres increases with f, the relation between f and the relative displacement δ is non linear. For small deformations, the first solution of this problem was given by Hertz [18]:

$$f = f_1 \delta^{3/2} \tag{1}$$

where f_1 is a function of the elastic moduli and the radii R_1 and R_2 of the spheres:

$$f_1 = K(1/R_1 + 1/R_2)^{-1/2} \tag{2}$$

and

$$1/K = 3/4((1-\nu_1^2)/E_1 + (1-\nu_2^2)/E_2) \tag{3}$$

E_i and ν_i are respectively the Young and the Poisson moduli of the particle i. Mindlin [19] studied how the Hertz solution is modified, when a tangential force and Coulomb's friction are introduced in the problem. He showed that the relation between f and δ is still non linear and depends on the history of the surface of contact. $f(\delta)$ remains a power law characterized by an exponent μ which does not significantly differs from the value $\mu = 3/2$.

3 Oedometric compression

3.1 Material and method

The aim of our experimental investigation is to determine the macroscopic force law $F(\varepsilon)$ between the imposed deformation ε and the measured force F, in polydisperse assemblies of spheres. Each sample is submitted to cycling deformations spanning between $\varepsilon = 0$ and $\varepsilon = \varepsilon_{max}$, at a constant compression speed ν. The oedometric procedure consists in imposing a vertical compression with fixed lateral boundaries. We investigate, on the characteristic curve $F(\varepsilon)$, the influence of speed, of wall effects as well as an increase of the maximum applied deformation ε_{max}. We include in this chapter a specific experimental study on the compression of a single sphere onto a plane. This study will be useful in the analysis of the packing compression results.

3.1.1 Material

The very soft spheres we use to make packing, are a partially neutralized poly(acrylic) acid gel swollen in salty water. These particles are from industrial origin and are synthetized in inverse emulsions of water in oil, stabilized by agitation (for applications as superabsorbants). After drying, the diameter d_d of the particles varies between few tens and few hundreds of microns. The volume of the gel varies in a reversible manner with the salinity of the solution in which it is immersed. The swelling ratio Q which is defined as the ratio of the volumes of the gel swollen in equilibrium (V_s) and in the dry (V_d) state ($Q = V_s/V_d$), represents the absorbency of the solution by the gel. We have measured the variation of Q with the salt concentration C_s of the solution by optical microscopy. The results are reported in Figure 1a. The neutralization degree of

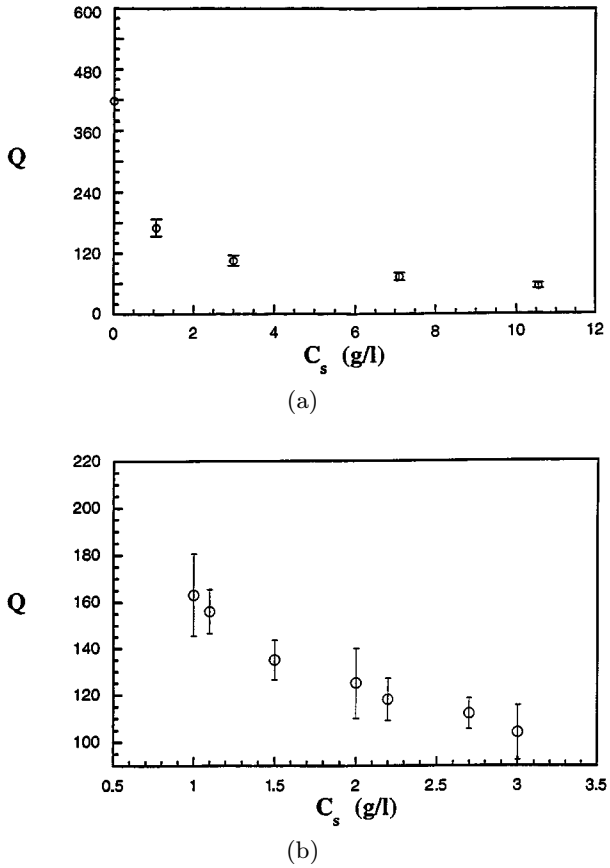

Fig. 1. Variation of the swelling ratio of the gel spheres with the salt concentration. (a) For 1 g/l $< C_s <$ 12 g/l; (b) for 1 g/l $< C_s <$ 3 g/l.

the gel, which is the rate of neutralized acid groups on the polyelectrolyte chains, is very high (about 75%). Therefore the values of Q (if C_s is not too high) are much greater than for neutral gels. We find a decrease of Q when C_s is increased. Note that this qualitative behavior was previously found by Schosseler *et al.* for gel spheres [20], and for monolithic gels [21]. The swelling ratio Q is apparently greater for beads than for monolithic gels of the same neutralization degree [21]: because in the former preparation, the polymeric concentration is higher and the reticulation degree is much weaker. In all the experiments we have performed, we have: 1 g/l $< C_s <$ 3 g/l. In these conditions, Q is always greater than 100. The density of a swollen particle ρ_s is estimated in the following way: the density of the dried gel ρ_d is measured by helium picnometry; we find $\rho_d = 1.5$ g/cm^3. Note that because the particles are slightly porous, when we try to deduce the apparent volume V occupied by a dried sphere (*i.e.* the volume of the gel and the porous volume inside the particle) from its weight and the dried density ρ_d, we obtain a small underestimation of V. Defining ρ_0 to be the density of the salty solution, we find: $\rho_s - \rho_0 < 0.006$ g/cm^3. Therefore, the role of the gravity in our packings is very weak and our system can be considered as almost isotropic at the beginning of every experiment. Figure 2 is a photograph of gel spheres swollen in brine. We see that the connection between two spheres in contact is tangential. This shows the absence of adhesion between the particles [22]. Due the presence of counterions near the polyelectrolyte chains at the surface of the gel, and to ions in the salty solution, the electrostatic repulsive forces between the particles are short range. They are negligible compare to the compression force F.

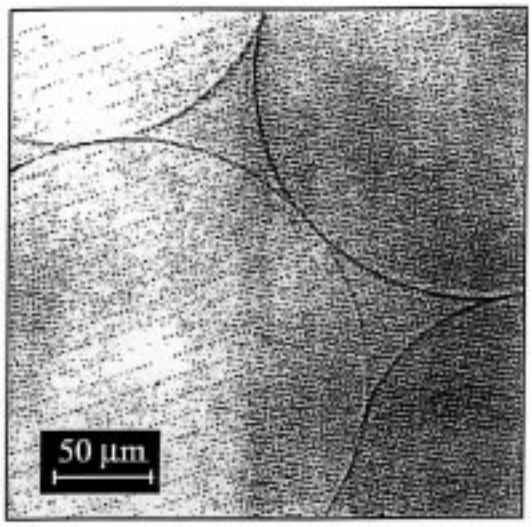

Fig. 2. Photograph of spheres swollen in a salty solution ($C_s =$ 3 g/l).

3.1.2 Samples preparation

The experiments of oedometric compression are performed on two sets of particles obtained after sieving of the dried product. The mean size of the particles is respectively equal to 307 μm and 380 μm. We simply estimate the value of the polydispersity s as:

$$s = 2(D_{max} - D_{min})/(D_{max} + D_{min}) \qquad (4)$$

where D_{max} and D_{min} are the nominal values of the mesh sizes of the sieves into which the particles are collected. Note that s calculated from equation (4) is an underestimation because it does not take into account dispersion in the sizes of the meshes for each sieve (which is not precisely known). Due to the fact that the mechanical behaviour of a packing may strongly depend on its history of construction, we prepared all the packings using the same procedure. First, the dried samples are weighted, and then, they are swollen in salty water ($C_s = 3$ g/l). The final equilibrium mean diameters of the particles hence obtained are 1.45 mm and 1.8 mm, and the estimated value of the polydispersity s is respectively 12% and 25%. In order to eliminate the residual dust, the solution is continually regenerated until the samples are entirely washed. The packings are prepared by pouring altogether the beads, immersed in the salty solution, into a cylindrical porous cell made

of stainless steel. During the filling procedure, the main part of the solution surrounding the particles always flows throughout the porous cell. This collective mode of construction is known to produce local arches in 2D and 3D dry packings. Since the motion of the salty solution around the spheres induces rearrangements in the packing, the number of local arches initially created in the system can be reduced, in a large extent, when the porous cell containing the drained sample is immersed once again into the solution before the onset of compression. The friction between the walls of the cell and the particles is responsible for the presence of arches which can partly hinder the transmission of forces through the packing. In order to reduce this effect, we use a cylindrical cell with a diameter equal to the height [23,24] ($H_c = D_c = 45$ mm). Since the size of the cell pores are much smaller than the swollen gel spheres, the porous walls of the cells can be considered as smooth at the scale of the particles.

The volume fraction η of our packings in brine is measured in the following way: a given mass of the dried product is initially swollen in brine ($C_s = 3$ g/l) and then poured into a test tube, then the total volumes of the swollen beads and the interstitial solution are measured. Knowing the equilibrium swelling rate of the particles ($Q = 100$) and estimating their dried volume using the apparent density ρ_d, we find the volume occupied by the swollen particles. We determine the initial volume fraction: $\eta = 0.57 \pm 0,027$. Note that Onoda and Liniger [25] have found that the volume fraction is $\eta_{min} = 0,55$ for packings of monodisperse spheres embedded in a liquid of equal density. This value represents the minimum density of a loose packing in the absence of buoyancy forces. Keeping in mind the fact that our system is polydisperse, we nevertheless deduce from this result that before compression the packing is very loose. Note that we can also deduce from the measured value of η that the number of particles n in our packings will not exceed 10 000 (if the cell is initially full).

3.1.3 Experimental technique

The experimental setup is shown in Figure 3. The porous cell which contains the sample is attached on a support S fixed on a plate which can be moved in the x, y and z directions. Two manual micrometric screws allow the motion in the x and y directions. A vertical displacement z at a constant speed ν is performed by a direct current motor. In our system, ν can be varied between 0.3 mm/min and 3.3 mm/min. A displacement sensor (of sensibility $\Delta z = 50$ μm) is fixed on the support and provides an electrical tension proportional to z (Fig. 4). A piston P is attached to an electromagnetic balance B which is placed on a rigid frame. Before starting each experiment, the cell is moved until its upper part reaches the piston. Then, using micrometric screws, a coincidence between the axis of the cell and the piston is obtained. The diameter of the piston is slightly smaller than the inner diameter of the cell in order to avoid friction with the walls of the cell as well as the crossing of a swollen sphere on the top of the packing through the gap between the piston and the inner part of the cell. Finally, the cell is immersed in the salty solution. A deformation of the packing in the vertical direction is obtained by moving the cell towards the fixed piston P. The feedback of the balance ensures that the piston stands stock-still during the measurement of the force F exerted by the spheres on the piston.

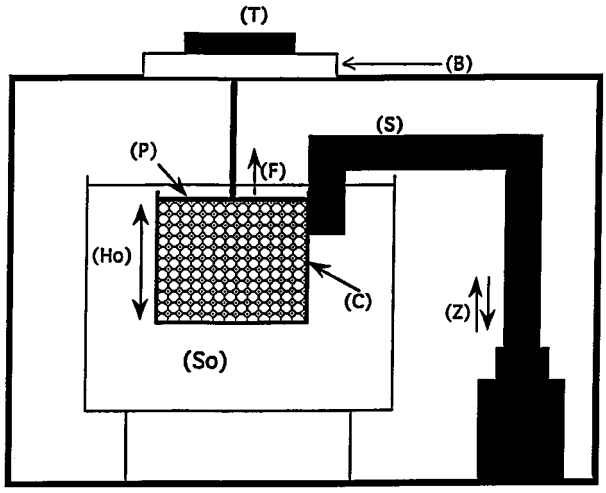

Fig. 3. Experimental setup for oedometric compression. C: cell; S: support; P: piston; B: balance; T: tare; F: force measured; S_0: salty solution; H_0: initial height of the packing; Z: vertical displacement of the cell.

In those opaque porous cells, it is not possible to measure the initial height H_0 of the packing. We therefore determine the origin of displacements from the onset of the compression force. The deformation ε of the system is defined respectively to a non deformed state. If H is the height of the deformed packing, we have:

$$\varepsilon = (H_0 - H)/H_0. \quad (5)$$

3.2 Local laws

In order to characterize the mechanical behavior of a particle, we perform an uniaxial compression experiment on a single swollen bead placed on an horizontal plane. Remark: this compression test is not an oedometric process since we do not impose a lateral constraint on the bead. A single sphere is placed in a glass cell full of brine and the experimental device, presented in Figure 3, is used to measure the force. The cell is placed on a support X which can be moved vertically towards the piston P by means of a manual micrometric displacement (Fig. 5). Then, we measure the relation between the deformation ε imposed to the particle and the related normal reaction force f, exerted by the particle on the piston P. The diameter of the non deformed particle d_s is determined when the contact between the sphere and the piston is established. The deformation of the sphere is given by: $\varepsilon = (d_s - h)/d_s$, where h is the distance between the piston P and the lower side of the cell during the compression. We have verified that

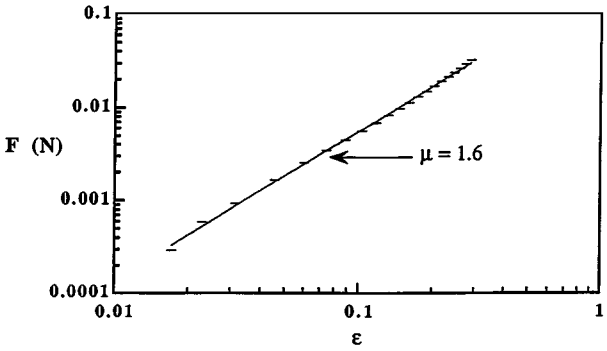

(a)

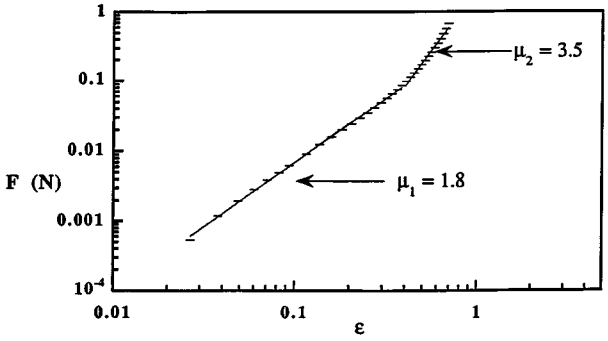

(b)

Fig. 4. Log-Log plot of the variation of the force with the deformation for a gel bead submitted to an uniaxial compression. (a) $\varepsilon_{max} = 30\%$; $d_s = 3.5$ mm. (b) $\varepsilon_{max} = 70\%$; $d_s = 4.5$ mm.

when P is moving, the forces due to buoyancy and to capillary effects are negligible.

When a gel particle initially swollen at equilibrium and maintained in its solvent is compressed, it can expell solvent. Nevertheless, the resulting volume reduction of the particle is negligible at small deformations [26]. Additionally, rearrangements of the polymer network due to a diffusion of the solvent inside the gel from the stressed zones to the unstressed ones can also occur [26]. Consequently, when a deformation is imposed to the gel, the reaction force first rapidly increases and then slowly decreases [26–28].

Experiments of uniaxial compression are performed on spheres of different diameters d_s (4 mm, 3.5 mm and 3.3 mm). The results for the variation of f with ε for the two deformation ranges investigated (0%–30% and 0%–70%) as reported in Figures 4a and 4b respectively. For $\varepsilon_{max} = 30\%$, the resistance to compression of a sphere is non linear and can be expressed in the form of a power law over the whole range of deformations ($2\% < \varepsilon < 30\%$). We have:

$$f = f_o \varepsilon^{\mu 1} \tag{6}$$

with $\mu_1 = 1.6 \pm 0.1$. As this exponent is very close to the Hertz's one, we estimate the Young modulus E of the gel by making the following assumptions: in the limit of small deformations, and assuming that the gel remains incompressible during the compression (the Poisson modulus is then equal to 0.5) the prefactor f_0 is given by the Hertz's law (2, 3):

$$f_0 = 4Ed_s^2/9. \tag{7}$$

The different measured values for f_0 gives an estimation of the Young's modulus $E \sim 4.2 \times 10^4$ Pa. On the curve displayed in Figure 4b we observe for $\varepsilon \sim 40\%$ a crossover to a new behavior. For $\varepsilon > 40\%$ a new regime appears for which the $f(\varepsilon)$ characteristic can not be described satisfactorily by a power law. Nevertheless, the effective slope in a log-log plot yields a value around 3.5 for $40\% < \varepsilon < 70\%$. Remark that this exponent value is greater than Hertz's theoretical value. The large deformation regime measured on gel beads is characteristic of the highly compressed gel material and is probably due to an important deswelling of the gel which expells a large amount of solvent for $\varepsilon > 40\%$. Note that in some experiments we have evidenced, for $\varepsilon < 40\%$, an effective exponent slightly greater than the Hertz's one ($\mu_1 \sim 1.8$ for the results reported in Fig. 4b). This is probably due to the fact that during the time of a compression test, $T(T \sim 5$ min), the particle slightly deswell. We have performed experiments of force relaxation as a function of time on gel spheres swollen in brine and submitted to an uniaxial compression at a constant deformation [27]. They show that two relaxation processes occurs successively, characterized by two very different relaxation times. The shorter one, τ is of the order of the total duration of the compression test T for the determination of the local law. Knaebel *et al.* [28] attributed the shorter relaxation process in compressed gel beads to diffusion of the solvent inside the gel from the stressed zones to the unstressed ones, accompanied by a small deswelling of the particle. These authors performed sets of uniaxial compression experiments of duration T much smaller than τ, and at deformations smaller than 20%. They measured a local exponent value $\mu = 1.5 \pm 0.1$, and therefore verify with a good accuracy that the local behavior of the gel obeys to the Hertz law [29]. Nevertheless, since in our experiment we operate with a value of T comparable to τ, we still measure a local exponent μ_1 which does not strongly differs from the Hertz's one. Note also that in our experiments of oedometric compression the time of the compression phase remains comparable to τ.

3.3 Global behaviour

First we present the results obtained for the study of the stabilization of the $F(\varepsilon)$ cycles. Then, we study the effect of the compression speed, of the walls and also the influence of the maximum applied deformation on the stabilized $F(\varepsilon)$ characteristic.

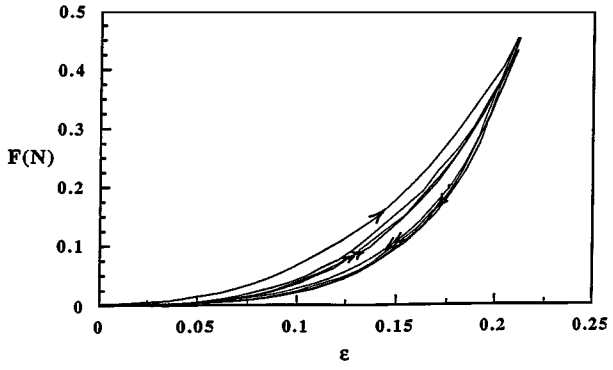

(a)

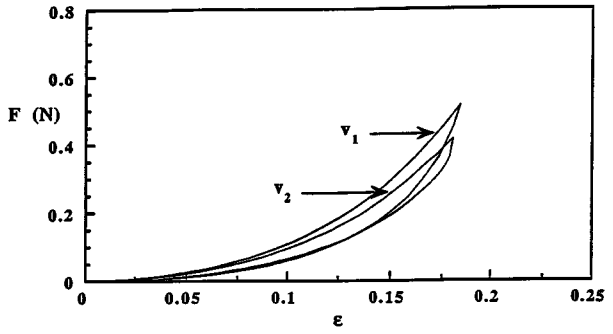

(b)

Fig. 5. (a) Variation of the force with the deformation for a packing submitted to several cycles of compression; $H_0 = 14.6$ mm; $v = 1.3$ mm/min; $\varepsilon_{max} = 20\%$. $\rightarrow$: first cycle. $\twoheadrightarrow$: fourth cycle. (b) Effect of the speed of compression on the variation of the force with the deformation (stabilized cycles). A packing is first cycly deformed at speed $v_1 = 3.3$ mm/min, and then at speed $v_2 = 0.33$ mm/min ($H_0 = 43$ mm).

3.3.1 Cycles of deformation - stabilization of the F(ε) characteristic

In Figure 5a we show the curve F(ε) obtained for a packing characterized by $H_0 \sim 14.6$ mm, $\nu \sim 1.3$ mm/min and $\varepsilon_{max} \sim 20\%$. This figure captures the main characteristics of the cycles of deformation. The response of the packing is non linear and all cycles are hysteretic. The amplitude of the hysteresis decreases when the number of cycles increases. For all samples, the stabilization of the characteristic $F(\varepsilon)$ occurs after only a few cycles (in Fig. 5a, after the third cycle). This result differs significantly from the behavior observed for packings of monodisperse hard spheres for which the stabilization of $F(\varepsilon)$ is reached around the fortieth cycle [30]. In packings of hard spheres, reorganizations and displacements of the particles occur during a large number of cycles before a steady behavior is reached. Apparently, for our systems of soft spheres, a stable configuration is reached more rapidly. The stabilization of the characteristic is reached even more rapidly at low speed (after 5 to 6 cycles for $\nu \sim 3.3$ mm/min and after 3 cycles for $\nu \sim 0.33$ mm/min): at large speed, the particles do not have enough time to reach their stable position during the two first cycles; at low speed, most of the rearrangements occur during the first cycle. In order to study the effect of the deformation speed on the amplitude of the hysteretic response, two kinds of experiments are performed. In the first one, two samples with nearly equal heights H_0 are prepared. Each of them is then submitted to cycles of deformation at speeds v_1 and v_2 respectively ($v_1 \sim 3.3$ mm/min and $v_2 \sim 0.33$ mm/min). In the second experiment, a sample of height H_0 is submitted successively to two sets of cycles at speed v_1 and v_2 respectively. Because the results obtained in both experiments are very similar, we report in Figure 5b those of the second one (stabilized cycles). Clearly the amplitude of the hysteresis increases with ν. Moreover, it is worth to notice that, although in this experiment, the configuration of the packing has been modified by the first series of cycles at v_1, his stabilized characteristic at v_2 is very similar to the one of the packing which has been compressed at v_2 only. Therefore, we conclude that the stable configuration reached by different packings of same initial height, prepared in the same conditions and submitted to cycles of compression with $\varepsilon_{max} \sim 20\%$ appears to be identical in a range $v_1 < \nu < v_2$.

3.3.2 Global law and speed effect

Now we analyze the compressive part of the stabilized cycle. In Figure 6a, we display in a logarithmic scale the global law obtained from the experiment presented in Figure 5a. The $F(\varepsilon)$ characteristic shows two regimes. Both can be empirically described by a power law:

$$F = F_o \varepsilon^m \tag{8}$$

m is defined as the compression's exponent. The first regime observed for $1\% < \varepsilon < 5\%$ is described by an exponent $m_1 = 1.5$ close to the local exponent μ_1. For $\varepsilon > 5\%$, the behaviour of the packing is non linear as it is governed by an exponent $m_2 = 2.3$ greater than the local one. When varying the speed of deformation ν between 0.33 mm/min and 3.3 mm/min, these two regimes are still observed and the values of m_1 and m_2 do not change significantly, within 9% for m_1 and 5% for m_2. These variations remain comprised within the experimental uncertainties. For this reason in all the experiments presented in the following part of this section, the value of ν was maintained equal to 1.3 mm/min. Considering all the experiments performed with sufficiently high packings (*i.e.* $H_0 > 7d_s$, see below) we find: $m_1 = 1.7 \pm 0.2$ and $m_2 = 2.5 \pm 0.2$. We interpret these results in the following way. In the regime of small deformations, m_1 is close to μ_1. Consequently the global law appears to be similar to the local one. The forces are transmitted through the packing by a network of force chains constituted by active contacts (*i.e.* contacts which transmit significant forces through the packing). Therefore, during the first stage of the compression, the number of active contacts is constant: either the network of force chains remains stable or it undergoes restructurations in such a way that

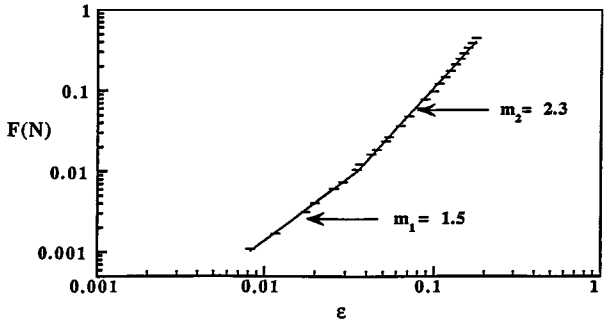

(a)

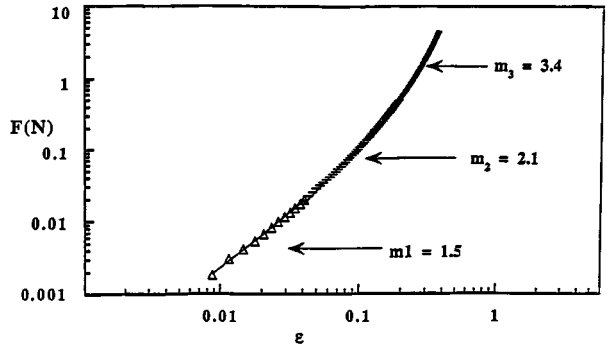

(b)

Fig. 6. (a) Log-Log plot of the variation of the force with the deformation (compressive part of the stabilized cycle) for the experiment reported in Figure 5a. (b) Large deformation behavior: log-log plot of the variation of the force with the deformation for a packing for which $v = 1.3$ mm/min, $\varepsilon_{max} = 37\%$, and $H_0 = 43$ mm.

the number of active contacts which break remains equal to the number of contacts which become active. We have tested, using a simple scaling argument, if the relevant force chains could be quasi linear. In this case, it is simple to estimate a scaling behavior such that:

$$F_0 \sim N f_0/(H_0/d_s)^{3/2} \tag{9}$$

where N would be the number of the nearly vertical force chains joining the piston and the lower part of the cell, and H_0/d_s the mean number of particles in a vertical chain. In fact our experimental outcome seems to contradict this simple viewpoint. We have determined for experiments performed for different initial heights H_0, the value of N given by equation (9) and the values of N hence calculated are very different. Additionally, they correspond to a density of linear chains greater than that obtained for close packing of linear chains. This result is not very surprising because in an oedometric experiment, the condition of zero lateral displacement imposes that normal forces are transmitted to the vertical wall of the cylindric cell by vaults. Nevertheless, it remains not obvious to understand why, in a disordered packing, we find a compression's exponent close to the local one. When the deformation increases, the mechanical contacts between spheres are still described by the Hertz's law, but the number of active contacts increases with the applied deformation (consolidated regime [23]). These two regimes have also been observed experimentally by Travers [31] on bidimensional (2D) ordered packings of equal cylinders of plexiglass submitted to an oedometric compression. The consolidated regime was found to be governed by an exponent $m_2 \sim 3.9$ higher than the local exponent (which was measured experimentally for cylinders [23]). The disorder of contact in these systems was of small amplitude and was due to a small distribution in the radii of the cylinders and to the rugosity of their surface. Travers *et al.* also showed that when increasing the disorder of the packing (obtained by introducing an increasing fraction of larger cylinders), the exponent m_2 decreases until it reaches the value 2.7 for maximal disorder [23]. For ordered packings of very deformable cylinders of rubber, Travers found that the exponent characterizing the global law is comparable to the local one [4]. This is due to the fact that the scale of the heterogeneities being always smaller than the scale of the imposed deformations, all the contacts between cylinders are active. Both regimes mentioned above are recovered in numerical simulations of a scalar transport problem in two dimensions [32]. Moreover, for crystals of monodisperse steel spheres, Duffy and Mindlin [33] found $m = 2$ for the consolidated regime; and this value is also currently obtained in compression experiments on dry sands [34].

3.3.3 Wall effects

2D packings of identical particles present a general trend towards order. In 3D packings of identical spheres, the flat wall can generate an orientational order over a short distance that depends on the mode of construction of the packing [35]. This order is impossible in 3D packings which present a weak dispersion in the sizes of the particles [35]. We try now to test the presence of wall effects in our disordered packings of soft spheres. Oedometric compressions where performed on packings of spheres with a diameter around 1.5 mm for which H_0 has been varied between 5 mm and 43 mm. Two different situations are studied: in the first case, the packings were built from the flat wall of the porous cell described above; in the second case, the bottom of the porous cell has been recovered by a layer of perfectly identical glass spheres glued on it in order to obtain a roughness at the scale of the gel spheres (the diameter of the glass beads was approximately twice the mean diameter of the swollen spheres). In Figure 7 the variations of the exponents m_1 and m_2 with H_0 are reported. In all experiments ν was equal to 1.3 mm/min. In both cases and for $H_0 > 10$ mm (*i.e.* for $H_0/d_s \sim 7$) m_1 and m_2 fluctuate around a mean value equal to $m_1 = 1.7$ and $m_2 = 2.5$ respectively. The amplitude of the fluctuations is smaller than the experimental uncertainties. The deformation ε_t at which the transition between the two regimes occurs fluctuates between 4% and 6%. For $H_0 < 10$ mm, an increase of ε_t and of the values of m_1 and m_2 is observed in the case of a flat wall (for $H_0 \sim 5$ mm, $m_1 \sim 2.2$,

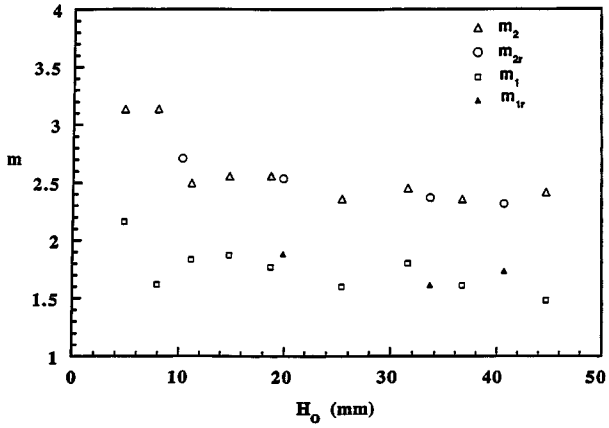

Fig. 7. Wall effects: variation of the two exponents describing the global law $F(\varepsilon)$ with the initial height of the packing H_0 for $\varepsilon_{max} = 20\%$. m_1 and m_2 are the results obtained when the bottom of the cell is flat, whereas m_{1r} and m_{2r} refer to the situation where a roughness has been created on the lower part of the cell by gluing glass beads of diameter $D = 2d_s$ on it.

$m_2 \sim 3.25$ and $\varepsilon_t \sim 14\%$). The same qualitative result was obtained by Travers *et al.* [23] on 2D ordered packings of dry cylinders: they found that the macroscopic exponents m_1 and m_2 increase when H_0 decreases.

3.3.4 Large deformations

Now we study the influence of an increase of the maximal applied deformation ε_{max} on the global law $F(\varepsilon)$. In Figure 6b we display in a log-log representation results obtained for an amplitude of deformation $\varepsilon_{max} \sim 37\%$ for a packing for which H_0 is equal to 43 mm. Besides the consolidation regime and the consolidated one, a third regime appears on the curve $F(\varepsilon)$ at large deformation ($\varepsilon > 20\%$); it can approximatively be described by a power law with an exponent $m_3 \sim 3.4$. This exponent is comparable to the one describing the local law for $\varepsilon > 40\%$ (*cf.* Fig. 4b, $\mu_2 \sim 3.5$). This result can be explained as follow: when ε approaches 20%, because of the large deformability of the particles all the contacts between the beads are active. And when the deformation of the system proceeds, most of the active contacts correspond to very deformed particles. Consequently the exponent m_3 is close to μ_2. The transition between the consolidated regime and the third one where the behaviour of the packing is dominated by the contribution of the very deformed particles occurs at a deformation $\varepsilon_s \sim 20\%$. Note that this crossover value is smaller than the value obtained for the compression of one particle ($\varepsilon \sim 40\%$). This is due to the fact that for a given deformation, the forces exerted on one particle in the packing are different from those it undergoes in an uniaxial compression. Moreover, when the displacement imposed to the packing become comparable to the initial heterogeneity, close to $d_s^{max} - d_s^{min}$, all the mechanical contacts are established in the system (d_s^{max} and d_s^{min} are respectively the diameters of the largest and the smallest particles). This threshold corresponds to a deformation ε_s:

$$\varepsilon_s = 2(d_s^{max} - d_s^{min})/(d_s^{max} + d_s^{min}) \qquad (10)$$

hence ε_s appears to be closely related to the polydispersity s of the system. The latter is estimated to 12% for the two packings used in this study, but we know (see Sect. 3.1.2.) that this value is very approximate und probably underestimated. The right polydispersity is therefore in the system of Figure 6b probably closer to 20%. A transition to a regime of large deformations has also been observed in numerical simulations in 2D [36] and in experiments performed on 3D packings of stainless steel beads [33]. In both cases, the deformation at which this regime appears is comparable to the polydispersity of the system: $\varepsilon_s/s \sim 1$. Finally, we observe a small decrease of the value of m_2 for the large deformed systems, when compared to systems where $\varepsilon_{max} < \varepsilon_s$. This suggests that the additional rearrangements taking place at large deformations modify the dynamics of the increase of the number of active contacts in the consolidated regime.

4 Isotropic compression

In an experiment of oedometric compression, the deformation procedure can induce an anisotropy of the network of active contacts. Additionally, the friction between the walls of the cell and the particles can partly hinder the transmission of the forces through the packing. In order to eliminate these two effects, we also perform isotropic experiments. First we introduce the isotropic compression procedure. Then we present the experimental results. Finally these results are discussed and compared to those obtained in the oedometric compression experiments.

4.1 Procedure

The apparatus used for this study, as well as the procedure of preparation of the samples are the same than the one used in the oedometric compression tests (see Fig. 3 and Sect. 3.1.2.). The principle of the isotropic compression is shown in Figure 8. A packing of spheres, initially swollen in a solution of salt concentration C_{s1}, is placed in a rigid cylindrical porous cell which is closed in its upper part by means of a piston P attached to the electromagnetic balance. Both are immersed in the solution of preparation. Initially, the packing does not occupy all the inner volume of the cell. A progressive dilution of the solution induces a swelling of the particles until they occupy the whole cell's volume for a salt concentration C_{so}. When the dilution process goes on, the particles placed in a constant volume are prevented from swelling at equilibrium. Consequently, they exert on each other forces which are transmitted through the packing and are experienced on the walls of the cell. Thus, for each concentration C_s, we measure the vertical component F of the resulting force exerted on the piston P, at equilibrium. By imposing cycles of swelling and deswelling (respectively by dilution and

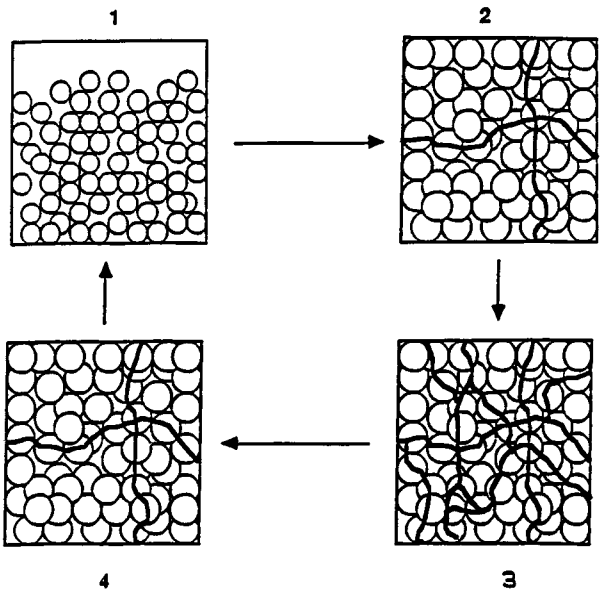

Fig. 8. Principle of an experiment of isotropic compression. (1) Initially the spheres swollen at a salinity C_{s1} do not occupy all the accessible volume of the cell; (2) then the solution is diluted and the particles swell. Forces are transmitted through the packing when $C_s > C_{s0}$, which corresponds to the rigidity threshold; (3) when the dilution goes on, the swelling of the beads at equilibrium is hindered, and the network of forces in the system densifies; (4) when C_s decreases, the particles deswell, and rearrangements take place in the packing. The force exerted on the upper part of the cell is measured as a function of the salinity, when cycles of swelling and deswelling are imposed to the system.

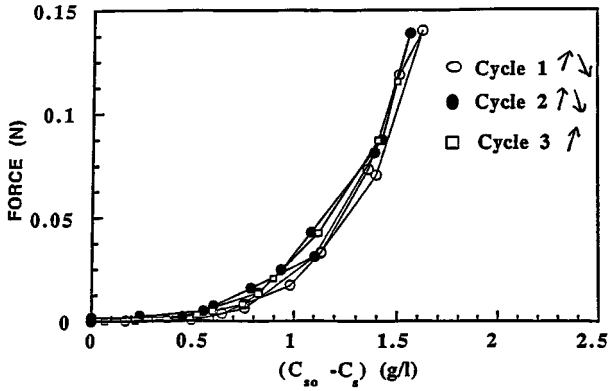

(a)

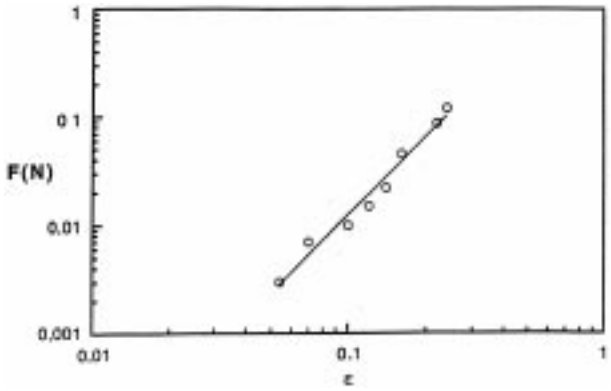

(b)

Fig. 9. Isotropic compression of a packing of about 3600 particles submitted to 2.5 cyles of deformation. (a) Variation of the force with the salt concentration; $C_{so} = (2.86 \pm 0.01)$ g/l. (b) log-log plot of the variation of the force with the deformation for the compressive part of the stabilized cycle.

concentration of the solution), rearrangements are generated in the packing. The salt concentration C_{so} beyond which the measured forces are not zero corresponds to the rigidity threshold of the packing.

4.2 Experiments

Two experiments were carried out on two different samples in a rigid cylindrical porous cell ($H_c = D_c = 24$ mm). $C_{s1} \sim 3$ g/l. For the two samples $H_0 \sim 21$ mm, however the mean diameters of the particles d_s are different and consequently their number n are different ($n \sim 11\,000$ for $d_s = 1$ mm and $n \sim 3600$ for $d_s = 1.45$ mm). Note that the value of H_0 is here very approximate, because it is obtained from the weight of the dried samples and the estimated volume fraction η of the packings of swollen particles (see Sect. 3.1.2.). C_s is measured by means of the proportioning of the solution around the cell with a solution of $AgNO_3$ of normality $N = 0.1$. For each ΔC_s, the time to reach equilibrium is related to the time of diffusion of the solvent into the gel beads which depends of the macroscopic diffusion coefficient D_c [20]. As $D_c \sim d_s^2$, the duration of an experiment comprising two or three cycles is then about five days for our millimetric particles. The elastic properties of the gel beads *a priori* vary with the salt concentration C_s. In order to study this variation, uniaxial compression experiments are performed on gel cylinders successively swollen at equilibrium at different salt concentrations [27] (their chemical composition is very close to that of the gel spheres). We find that their shear modulus present no significant variation with C_s, for 1 g/l $< C_s <$ 3 g/l.

4.3 Results and discussion

In Figure 9a are reported the results for the characteristic $F(C_{so} - C_s)$ for $n \sim 3600$ (the results obtained for $n \sim 11\,000$ are very similar). We find that $C_{so} = 2.86 \pm 0.01)$ g/l. The cycles show a small hysteresis and the stabilization is reached after the second cycle. In order to analyze these results and to compare them to those obtained in the oedometric compression, it is necessary to know the relation between the control parameter $(C_{so} - C_s)$ and the global deformation of the packing ε_g. We define ε_g respectively to the non deformed state, like

for the oedometric compression experiments:

$$\varepsilon_g = (V_{eq}(C_s) - V_{eq}(C_{so}))/V_{eq}(C_s). \quad (11)$$

$V_{eq}(C_s)$ is the volume that the packing would occupy (spheres and interstitial solvent) if the particles were allowed to swell at equilibrium at C_s. Note that $V_{eq}(C_{so})$ also corresponds to the volume of the cell, V_c. $V_{eq}(C_s)$ can be expressed as:

$$V_{eq}(C_s) = nV_dQ(C_s)/\eta_1 \quad (12)$$

and

$$V_{eq}(C_{s0}) = nV_dQ(C_{so})/\eta_o = V_c \quad (13)$$

where V_d is the mean volume of the spheres in the dry state. η_1 and η_o are the volume fractions of the packing in the non deformed state at C_s and C_{so} respectively. Then the experiment can be viewed as the result of a succession of isotropic compressions performed on packings initially swollen at equilibrium at different salt concentrations, then piled under the same conditions in cylindrical cells of same aspect ratio ($H_c = D_c$) and finally compressed isotropically until they occupy the constant volume V_c. One can reasonably assume that the volume fraction in the undeformed state defined above is independent of the salt concentration: $\eta_1 = \eta_o$. Following (11, 12, 13) ε_g is then given by:

$$\varepsilon_g = 1 - (Q(C_{so})/Q(C_s)). \quad (14)$$

We determine the values of ε_g from the values of $Q(C_s)$ measured in the salt concentration range 1–3 g/l (Fig. 1b). In Figure 9b we plot the log-log representation of the characteristic $F(\varepsilon_g)$ corresponding to the compressive part of the stabilized characteristic of Figure 9a. The behaviour is non linear. For $\varepsilon_g > 5\%$ the $F(\varepsilon_g)$ curves can be correctly fitted by a power law of exponent m_{iso}. For $\varepsilon_g < 5\%$, the lack of experimental points prevents the characterization of the behaviour at small deformations. This is due to the fact that the forces measured at smaller defomations are of the same order of magnitude as the experimental uncertainties. Considering the two experiments performed, we find $m_{iso} = 2.7 \pm 0.2$ over the deformation range 5%–24%. Note that m_{iso} is greater than the Hertz's exponent. Hence, the observed regime corresponds to the consolidated one. Moreover, m_{iso} is very close to the mean value of the exponent m_2 which describes the consolidated regime in the oedometric experiments ($m_2 = 2.5 \pm 0.2$) and also to that obtained by Travers for 2D disordered packings of cylinders of plexiglass submitted to oedometric compression ($m_2 = 2.7$) [23]. The fact that the global exponent in the consolidated regime appears to be very close in our 3D experiments and in the 2D experiments of Travers [23] may look *a priori* surprising. It could be understood in the following way: in this intermediate regime, the compression law is controlled by the increase in the number of active contacts and this can be viewed, in a mean-field description, as independent of the spatial dimension and of the local compression laws. However, because of the lack (to our knowledge) of other compression experiments on different model packings in 2D as well as in 3D, this explanation must be considered as a very tentative one.

5 Summary and conclusions

Mechanical properties of packings of deformable spheres made of a polyelectrolyte gel are studied experimentally. The particles are immersed in brine and have the property to swell or shrink with respect to salt concentration. Oedometric compression experiments are performed on the system, by imposing cycles of deformation ε at a constant concentration and compression rate. The resulting average force F on the piston is measured and after few strain cycles, a compression law is found which can be described empirically by a non-linear relationship of the type: $F \sim \varepsilon^m$. In parallel, experiments are performed to obtain the local compression laws of a single sphere between two planes. For many experiments on the granular assemblies, under various compression speeds, three regimes are observed when ε is increased. For small ε's an exponent $m_1 \sim 1.7 \pm 0.1$ (close to the local exponent in the small compression regime) is measured. This behavior is reminiscent of a behavior which was evidenced either experimentally [4] or numerically [37] in two dimensions for compact and regular assemblies of dry grains. For this regime (sometimes called the "consolidation regime" [23]) an interpretation was given and tested numerically [37]: it corresponds to a situation where, in the average, the number of active contacts is roughly constant. Interestingly in our case, we work in a situation where geometrical disorder is present as well as a rather loose packing. For higher strain ε, we obtain a cross-over to a compression law with an exponent: $m_2 \sim 2.5$. Such a cross-over to a compression law with a higher exponent m was also evidenced previously [31]; nevertheless the value of m depends on the system studied. In some instances, this was called the "consolidation regime" [31] probing a situation where the number of active contacts increases along with the compression. Note that an identical value of $m_2 \sim 2.5$ was found in a 2D experiment with a disordered array of dry cylinders [23]. At large deformations, we measure an exponent which identifies with the local one at large ε's: $m_3 \sim 3.5$. Such a behavior was probed on computer simulations of regular arrays of discs in 2D [36]. It corresponds to a situation where, due to the high compression state, all the contacts are active. Nevertheless, note that in the numerical case, the local law is still of the Hertz's type and thus, $m_3 = 1.5$ is found [36]. A second series of experiments of isotropic compression is performed by cycling the salinity of the solution, where the particles successively swell and deswell in a cell of constant volume. In this case, a non-linear response is also probed, corresponding to the intermediate regime of deformation $F \sim \varepsilon^{m_{iso}}$, with $m_{iso} \simeq m_2$. Note that for practical experimental reasons we could not access to the very small and very large deformation ranges and probe the other regimes. In conclusion, these experiments on packings of very deformable and polydisperse spheres in a saturated

situation show general mechanical properties which are quite robust and similar to other experiments on model dry granular assemblies. On the other hand, properties such as the exact values of the effective compression exponents, the ranges of the different compression regimes etc., do not show this type of universality. And it is still an open question to understand the relevant features of the compression dynamics, the boundary conditions, the history of construction of the packings to have a full mechanical picture of the passage between the local granular interactions and the global mechanical behavior.

We thank S.J. Candau, F. Schosseler, J.P. Munch and S. Roux for very helpful discussions. The authors dedicate this work to J. Bastide.

References

1. R.L. Brown, J.C. Richards, *Principle of Powder Mechanics* (Pergamon Press, New York, 1966).
2. *Powders and Grains* (Durham 18-23 may 1997), edited by R.P. Behringer, J.T. Jenkins (Balkema, Rotterdam, 1997).
3. H.M. Jaeger, S.R. Nagel, R.P. Behringer, Rev. Mod. Phys. **68**, 1259 (1996).
4. T. Travers, D. Bideau, A. Gervois, J.P. Troadec, J.C. Messager, J. Phys. A **19**, 1033 (1986).
5. C.H. Liu, S.R. Nagel, D.A. Schecter, S.N. Coppersmith, S. Majumdar, O. Narayan, T.A. Witten, Science **269**, 513 (1995).
6. B.J. Miller, C. O'Hern, R.P. Behringer, Phys. Rev. Lett. **77**, 3110 (1996).
7. F. Radjai, M. Jean, J.J. Moreau, S. Roux, Phys. Rev. Lett. **77**, 274 (1996).
8. S. Ouagenouni, J.N. Roux, Europhys. Lett. **39**, 117 (1997).
9. C. Eloy, E. Clement, J. Phys. I France **7**, 1541 (1997).
10. J.P. Bouchaud, M.E. Cates, P. Claudin, J. Phys. I France **5**, 639 (1995).
11. S.F. Edwards, R.B.S. Oakeshott, Physica D **38**, 88 (1989).
12. R.M. Nedderman, *Statics and Kinematics of Granular Materials* (Cambridge University Press, Cambridge, 1992).
13. S.B. Savage, *Powders and Grains*, Durham 18-23 may 1997, edited by R.P. Behringer, J.T. Jenkins (Balkema, Rotterdam, 1997), pp. 185-194.
14. T. Travers, D. Bideau, A. Gervois, J.C. Messager, J.P. Troadec, Europhys. Lett. **4**, 329 (1987).
15. N.A. Clark, B.J. Ackerson, Phys. Rev. Lett. **44**, 1005 (1980).
16. C. Allain, C. Amiel, Ann. Chim. **17**, 91 (1992).
17. D. Senis, C. Allain, Phys. Rev. E **55**, 7797 (1997).
18. H. Hertz, J. Reine und Angewandte Mathematik **92**, 156 (1895).
19. R.D. Mindlin, *Proc. 2nd US Natl. Congr. Appl. Mech.* (Ann Arbor, Michigan, 1954).
20. F. Schosseler, P. Mallo, C. Cretenot, S.J. Candau, J. Disp. Sci. Techn. **321**, 321 (1987).
21. F. Schosseler, F. Ilmain, S.J. Candau, Macromolec. **24**, 225 (1991).
22. K.L. Johnson, K. Kendall, A.D. Roberts, Proc. Roy. Soc. London A **324**, 301 (1971).
23. T. Travers, Ph.D. thesis, Rennes, 1988.
24. Y. Ito, H. Kino, Powder Technol. **20**, 127 (1978).
25. G.Y. Onoda, E.G. Liniger, Phys. Rev. Lett. **64**, 2727 (1990).
26. A. Knaebel, Ph.D. thesis, Strasbourg, 1996.
27. T. Lachhab, Ph.D. thesis, Paris, 1994.
28. A. Knaebel, F. Lequeux, Polymer Gels and Networks **5**, 577 (1997).
29. A. Knaebel, S.R. Rebre, F. Lequeux, Polymer Gels and Networks **5**, 107 (1997).
30. L. Oger, Ph.D. thesis, Rennes, 1987; M. Ammi, Ph.D. thesis, Rennes, 1987.
31. T. Travers, M. Ammi, D. Bideau, A. Gervois, J. Lemaitre, J.P. Troadec, J.C. Messager, J. Phys. France **48**, 347 (1988).
32. H.J. Hermann, D. Stauffer, S. Roux, Europhys. Lett. **4**, 347 (1987).
33. J. Duffy, R.D. Mindlin, J. Appl. Mech. (ASME) **24**, 585 (1957).
34. S.N. Domenico, Geophysics **42**, 1339 (1977).
35. R. Ben Aim, Ph.D. thesis, Nancy, 1970.
36. J.N. Roux, in preparation.
37. J.N. Roux, *Powders and Grains*, Durham 18-23 may 1997, edited by R.P. Behringer, J.T. Jenkins (Balkema, Rotterdam, 1997), pp. 215-218.
38. G. De Josselin de Jong, A. Verruijt, Cah. Gr. Fr. Rheol. **2**, 73 (1969).
39. P. Dantu, *Proceedings of the 4th International Conference on Soil Mechanics and Foundations Engineering* **1** (Butterworths Scientific Publications, London, 1957), pp. 144; P. Dantu, Géotechnique **18**, 50 (1968).
40. I.D. Evans, A. Lips, J. Chem. Soc. Faraday Trans. **86**, 3413 (1990).
41. D. Groshans, A. Knaebel, F. Lequeux, J. Phys. II France **5**, 53 (1995).